Archives of Materials Science and Engineering

Volume 108
Issue 1
March 2021
Pages 5-15

International Scientific Journal
published monthly by the
World Academy of Materials
and Manufacturing Engineering

DOI: 10.5604/01.3001.0015.0248

Microstructure silica leached by NaOH from semi-burned rice husk ash for moisture adsorbent

D.Q. A'yuni [a], A. Subagio [b], H. Hadiyanto [a], A.C. Kumoro [a], M. Djaeni [a,*]

[a] Department of Chemical Engineering, Faculty of Engineering, Universitas Diponegoro
Jl. Prof. Sudharto Tembalang, Semarang, Central Java, Indonesia

[b] Department of Physics, Faculty of Science and Mathematics, Universitas Diponegoro
Jl. Prof. Sudharto Tembalang, Semarang, Central Java, Indonesia

* Corresponding e-mail address: m.djaeni@live.undip.ac.id

ORCID identifier: https://orcid.org/0000-0002-8002-6627 (M.D.)

ABSTRACT

Purpose: This work aims to study the water vapor adsorption property of fine silica particles from semi-burned rice husk ash. The semi-burned rice husk ash is selected as the raw material since it contains high silica and is easily found as a by-product of pottery furnace combustion.

Design/methodology/approach: The silica adsorbent from semi-burned rice husk ash was prepared through a sol-gel method using various NaOH concentrations. In doing so, the different pH precipitation was also observed. Here, the fine silica powder was obtained by pulverizing dry sol-gel. The product characterizations were conducted based on water adsorption capacity at different air relative humidity.

Findings: The results show no significant effects of different treatments in the extraction and gelation process. The fine silica particles exhibit large porous surfaces with agglomerated nano-sized particles that formed pores. This porous structure is related to the distributions of pore size of each sample, which mostly obey the mesoporous characteristics. From sorption isotherm, weak adsorbent-adsorbate bonding was observed and demonstrated multilayer adsorption of mesoporous materials.

Research limitations/implications: The study of water adsorption was carried out at room temperature, which can change at any time, even though has no significant effect on the humidity. However, it is needed to study the adsorption in an incubated area to receive a constant temperature.

Practical implications: The products namely silica prepared from semi-burned rice husk ash show a high moisture uptake, especially at a high relative humidity region. This property can be comparable with the other silica preparation methods. So, this product can be a highly potential adsorbent for air or gas dehumidification systems.

Originality/value: The silica-based semi-burned rice husk ash as a water adsorbent is more sustainable than commercial silica. This is a positive contribution to find a potentially develop water vapor adsorbent with good adsorption capacity. Besides, the synthesis process is a simple and low-cost process.

Keywords: Microstructure, Moisture adsorption, Silica, Rice husk ash

Reference to this paper should be given in the following way:
D.Q. A'yuni, A. Subagio, H. Hadiyanto, A.C. Kumoro, M. Djaeni, Microstructure silica leached by NaOH from semi-burned rice husk ash for moisture adsorbent, Archives of Materials Science and Engineering 108/1 (2021) 5-15. DOI: https://doi.org/10.5604/01.3001.0015.0248

1. Introduction

Adsorption is a mass transfer process that the molecule of components in fluids bounded in the surfaces of solid material called an adsorbent [1,2]. In general, there are two types of adsorption namely physical and chemical adsorption. The physical adsorption occurs by Van der Waals force that is unstable and releases low heat [2]. The adsorption is reversible where the reverse process is called desorption or releasing bounded substances from a surface of adsorbent [1]. The sorption process was applied for air dehumidification resulting in dry air with moisture content close to zero. Here, the water from the air was adsorbed by a material that has a high affinity to water such as silica, zeolite, a pillared clay, and alumina. After a certain time, the adsorbents were saturated with water. The adsorbents can be reused after the regeneration process by introducing heat to remove bonds water [3]. The air dehumidification by the solid adsorbents was studied to enhance the driving force for drying. With low moisture content in the air, the mass transfer of water from a product to air can be sped up at low or medium temperature that is very beneficial for heat-sensitive products such as protein, vitamins, and other active substances [4].

Silica gel, zeolite, and activated carbon have been widely used as adsorbers of water content in the air around products that that must be maintained in a drought environment [5-7]. These materials have been applied as adsorbents for decades relying on their porous structure and high surface area. Also, functional groups and surface properties of adsorbents are considered to influence the water vapor adsorption process, such as the presence of the oxygen functional group on the adsorbent surface as the polar/hydrophilic sites [8-10]. In zeolite, the adsorption capacity is determined by the Si/Al ratio as a constituent compound, while in silica, physical properties such as porosity are a general overview, as well as the number of hydrophilic sites which are considered sufficiently influential on the adsorption capacity of carbonaceous materials. In several studies, the reason for choosing these three adsorbents was the abundance of natural materials that could be used as a source of adsorbents such as natural zeolite, fly ash [11], volcanic ash [12], silica sand, husks [13], coffee-shell [14], and bamboo [15]. Mostly, the adsorption uptake (a mechanism) of each adsorbent showed different characteristics that have been represented as some types of adsorption isotherms as a function of relative pressure or humidity [16]. Zeolites have a higher water vapor adsorption capacity at low pressure and humidity, while silica and activated carbon more likely to adsorb water at a higher condition [14,17,18]. Furthermore, some studies have observed zeolites, silica gel, and activated carbons performance as water vapor adsorbents potentially applied to food drying system [19,20].

The researchers have studied the properties of commercial silica as a water vapor adsorbent [21,22]. The report from Xin et al. [21] showed that salt-modified silica has a higher adsorption capacity than unmodified silica gel, although this result occurred only at relative humidity under 80%. In contrast, based on Negishi et al. [22] binder-modifications of mesoporous silica have no significant effect on the water adsorption capacity. Commonly, commercial silica was produced through high temperatures and pressure processes [23]. This high-energy requirement process is considered high-cost and less environmentally-friendly. Besides, to achieve a more sustainable approach, further exploration is needed to utilize a greener adsorbent source instead of the commercial silica.

Rice husk from paddy milling is one of the abundant natural materials that have great potential as a micro-structured silica water vapor adsorbent source. According to Bakar et al. [24], alkali/acid-cleaned-rice husks possessed a high porosity and OH groups on their surface. However, the bulk size of the adsorbent still has a low surface area, which is one of the considerations on choosing adsorbent materials. Hence, this issue can be solved by reducing the size of the adsorbent up to a nanometer or ultrafine. The smaller size can enlarge the surface area as well as increasing porous percentage in which speed up adsorption rate and improve water-loaded capacity.

In general, rice husk was calcined to produce rice husk ash that contained silica up to 90% and possessed a high surface area [24,25]. In several cases, the rice husk was processed through an acid leaching process before calcinations to remove dirt and other contaminants [24],

[26]. Then, to synthesize high-purity fine silica, the rice husk ash was extracted by the sol-gel method, which is a simple method with positive results [27]. The synthesized silica has a high purity in the micro until nanometer dimension, with polar groups at its surface, which are in the form of hydroxyls (oxygen-based functional groups). As observed, the sol-gel method is considered as a simple method with promising results to be applied as a water adsorbent, including: (a) high purity, (b) high surface area, (c) porous product, (d) particles in size of micro- until nanometers, and (c) containing polar sites. Moreover, this method is conducted at a low temperature, which means required less energy than flame spray pyrolysis [28] and less expensive than reverse emulsion that using surfactant as the stabilisator of emulsion [29].

In the silica preparation through the sol-gel method, exists a transition from sodium silicate solution into a more solid and porous product, namely silica gel. Hence, the sol-gel method consists of two stages: (a) solution preparation and (b) transition of solution (sol) into a gel (silica gel formation). In the solution preparation process, mostly, sodium hydroxide (NaOH) solution was utilized to obtain sodium silicate solution which is then reprocessed to become silica gel [25,30,31]. At this stage, a hydrolysis reaction occurs which is influenced by the molar ratio between the silica contained in rice husk ash and NaOH as a solvent. Meanwhile, at the gel formation stage, pH is one of the main roles because changes in pH value affect the precipitation of sodium silicate solution into silica gel. Therefore, the different concentrations of NaOH solution in the solution preparation step and different pH values of the gelation are examined by several characterizations, including morphological analysis, chemical group analysis, and adsorption properties analysis. This experiment used an extraction process to synthesis silica gel from semi-burned rice husk ash (SBRHA). The method was adapted from Zaky et al. who prepared the silica gel from semi-burned rice straw ash (SBRSA) [32]. This process has a higher efficiency than the previous process using the calcinations process. In the leaching process using NaOH, Zaky et al. [32] modified the stoichiometry of SiO_2:NaOH, reaction time, and temperature to calculate the percentage of silica dissolution efficiency. Further observation of the gelation process did not become the main purpose of their study. Thus, to obtain the optimum treatment in the silica synthesis from side product of rice/paddy, this research continues the modification using variations of pH in the gelation process. For the forward process to obtain micrometer silica powder, silica gel was dried and pulverized. The main objective of this work is to study the property of a new (potentially develop) water vapor adsorbent from semi-burned rice husk ash that has been synthesized by sol-gel method with different treatments.

2. Materials and methods

2.1. Materials

Semi-burned rice husk ash (SBRHA) was obtained from the furnace of pottery industry (burned at 300ºC for 24 hours) at Depok, West Java, Indonesia. Before the extraction step, SBRHA was cleaned from contaminants with a home sifter. The silica preparation was conducted using 1 N hydrochloric acid (HCl) with different concentrations of sodium hydroxide (NaOH) solutions ranging from 5.0 to 10.0 % (w/w).

2.2. Synthesis of micrometer sized silica

The synthesis process of microparticle silica consists of three main steps involving preparation of sodium silicate solutions, formation of silica gels, and preparation of silica powders. The first step was executed by mixing continuously and boiling SBRHA at 90ºC for 90 minutes under different concentrations of NaOH solution of 10.0, 7.5, and 5.0% w/w. The mass to volume ratio of SBRHA and all NaOH solutions were kept at 1:6 mass (gram) per volume (mL). Based on reaction (1), the reaction of solid SiO_2 with liquid NaOH happened as 1:2 stoichiometric ratio. In this case, the NaOH solution was excessive to increase the SiO_2 conversion [33]. During the process, the following reaction occurs:

$$SiO_2(s)+2NaOH(l) \rightarrow Na_2SiO_3(l)+H_2O(l) \quad (1)$$

After the mixture cooled down to room temperature, the SBRHA residue and filtrate were separated. This filtrate is a yellowish-transparent color sodium silicate solution that can be employed as silica gel source. The SBRHA residue was mixed again with sodium hydroxide solution in the same concentration and processed until filtration as the previous step.

The second step was the gel formation process with neutralizing sodium silicate using 1.0 N hydrochloric acid solution. The solution was stirred and titrated with hydrochloric acid gradually. The SBRHA treated by 10% (w/w) NaOH was neutralized until pH 7 to form gel called sample A. The procedure was repeated for SBRHA with

7.5% and 5.0 % (w/w) NaOH solutions where the gel products formed were called as samples B and C, respectively. The SBRHA treatment using 5.0% (w/w) NaOH was also titrated with 1.0 N HCl until pH 5. Here, the gel was formed that was called as sample D. So, the four gel samples with different treatment were resulted and characterized. During the HCl titration, the following reaction occurs:

$$Na_2SiO_2(l)+2HCl\ (l)\rightarrow SiO_2(gel)+2NaCl\ (s)+H_2O(l) \quad (2)$$

The formed gels were put in a closed jar at room temperature for a night. The gels were filtered and washed with deionized water until the clear gels were obtained. The cleaned gels were dried 80°C for 20 hours to produce white solids. The solids were pulverized to powder using a mortar and screened through 200 mesh sieve (75 µm) to obtain the microstructure silica grains.

2.3. Characterization of prepared samples

The morphology characterization was evaluated using scanning electron microscope (SEM, JEOL Ltd. JSM-5610). The adsorption of N_2 of samples was recorded with Quantachrome® ASIQwin™ (Quantachrome Instruments version 3.01) at 77 K. The chemical property of samples was also analysed using Fourier Transform Infrared Spectroscopy (FTIR) in order to identify the functional groups having affinity to water. The spectra were recorded by PerkinElmer Frontier Infrared Spectrometer version 10.03.06, with a resolution of 1 cm^{-1}.

2.4. Adsorption studies

The result of this study is proposed to observe how much moisture can be adsorbed at various adsorption conditions. Water vapor adsorption analysis on silica was carried out with reference to previous studies [34]. The samples were kept in the saturated salt solutions environment to be maintained at constant relative humidity (RH), confirmed by hygrometer in the system.

Five different salt solutions were prepared (Tab. 1) with the range of RH of 8.00-84.00% at a room temperature (assumed 30±2°C) [34,35]. Salts were dissolved in 100 mL of distilled water until saturated and reach an equilibrium relative humidity. The solutions were then transferred to a closed glass jar. Silica samples were placed on the aluminum foil-wrapped plastic plate and held on a plastic tube that is higher from the solution surface. The set-up description is displayed in Figure 1. Samples were weighed at 24-hour intervals to measure the mass change that occurred, which means an increase in the moisture content of the sample until the constant mass was obtained.

Table 1.
Relative humidity of different saturated salt solutions at 30°C

Salts	Relative humidity, %
NaOH	8.00
$CaCl_2$	24.00
NaCl	75.00
KCl	84.00

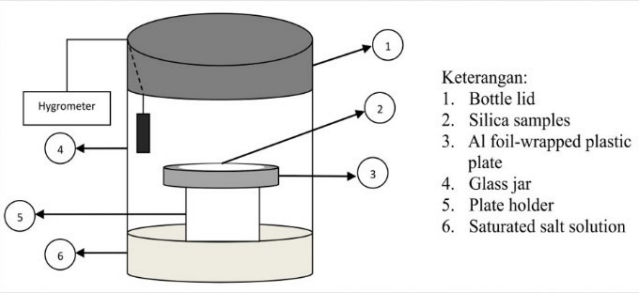

Fig. 1. Experimental set-up to study water vapor adsorption of samples

3. Result and discussion

3.1. Morphological analysis

According to the morphological characterization by SEM (Fig. 2), SBRHA sample shows an image of porous particles from bulk materials and a large component of agglomerated small particles in the spherical and rod form. These small particles are produced from the decomposition of rice husks after the burning process [36]. In comparison with reference [37], the treated rice husk ashes showed a wide porous of large particles with a minimum amount of agglomerated small particles. It is clearly shown from Figure 2a that silica from rice husk mixed with combustion carbon.

Figure 2b represents the SEM image of silica treated with a 10.0% concentration of NaOH solution (sample A). It appears that there are still many large-sized particles with a mixture of nano-sized particles agglomerating to form pores. There are also large pores with micrometer dimensions in the form of slits in large particles. The morphology of this sample looks more homogeneous,

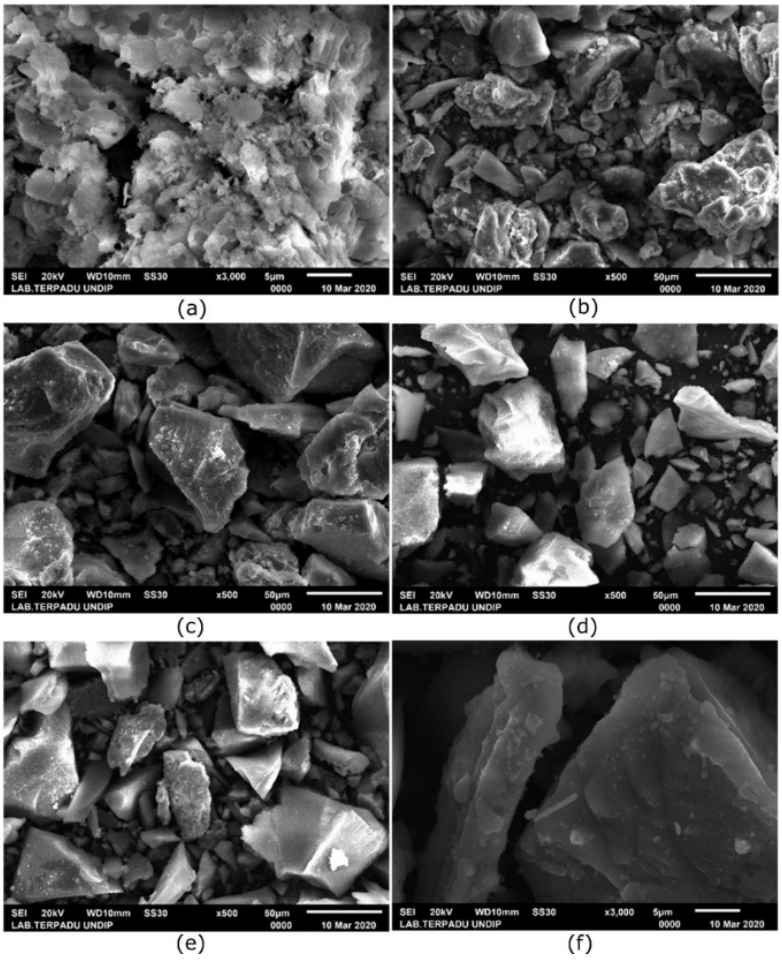

Fig. 2. SEM images of (a) SBRHA, (b) sample A, (c) sample B, (d) sample C, (e) sample D 500 magnification, and (f) sample D of 3000 magnification

although it is not the same size. The morphology of sample B and C (Fig. 2c and 2d) looks quite similar, although in size it appears that sample C is slightly smaller than sample B. The surfaces consist of large porous particles with a few agglomerated nano-sized particles. Even though when viewed from a macro perspective it is almost the same as sample C when viewed with magnification it is shown that sample D (Fig. 2e and 2f) is not a formation of agglomerated particles, but more likely to be large-shaped particles. Indeed, there are rod-shaped particles such as this also obtained by Joni, et al. [38].

3.2. N_2 sorption and pore size distribution

Generally, in most references, N_2 desorption was used to determine pore size distribution because of its thermodynamics equilibrium [39]. Neverthless, there is also a limitation in evaluating the pore size of the desorption curve, the occurence of cavitations in shrinking pores and occurs at a relative pressure of ~ 0.42 for N_2 at 77 K. Therefore, before observing the particle size distribution, the adsorption-desorption curve should be evaluated using the BJH (Barrett, Joyner, and Halenda) method. As a representative, N_2 adsorption-desorption characterization was conducted to sample B and C (Fig. 3).

The adsorption-desorption curves are shown in Figure 4. This curve shows a similar distribution, but a peak at D~4.8 nm for sample C and peak at D~1.7 nm in sample B. The absence of peak in the adsorption curve exhibits the presence of obstructed pores that have been used to measure the volume [40]. Based on these results, desorption is used for a particle size distribution analysis. From the desorption process, the pore size distribution of the two samples is from

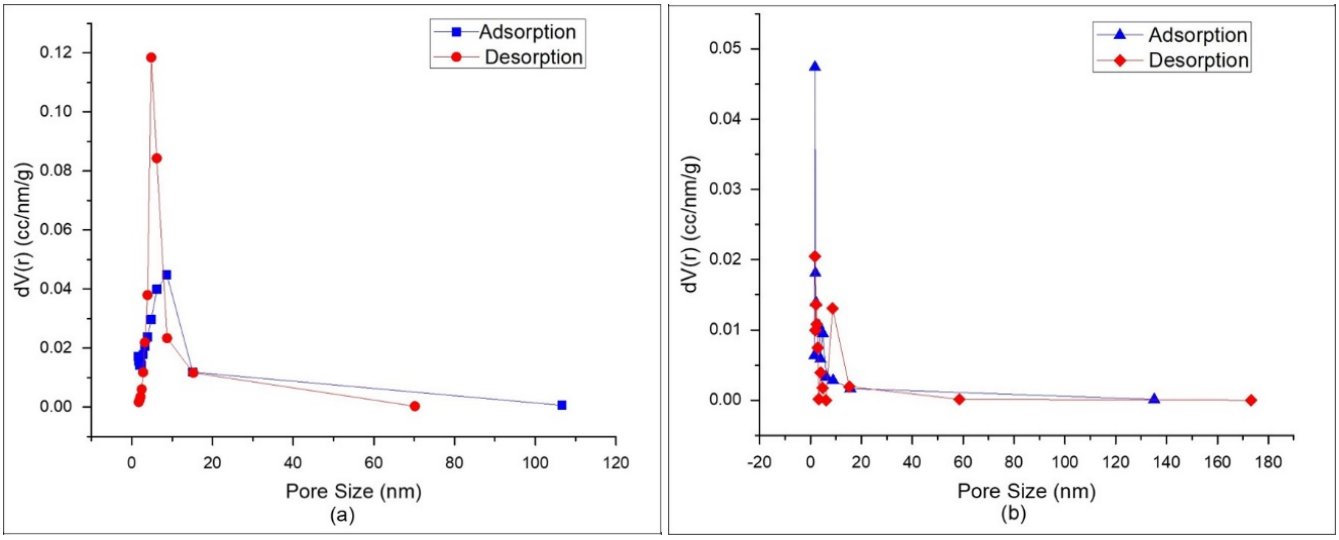

Fig. 3. Pore size distribution of (a) sample B and (b) sample C

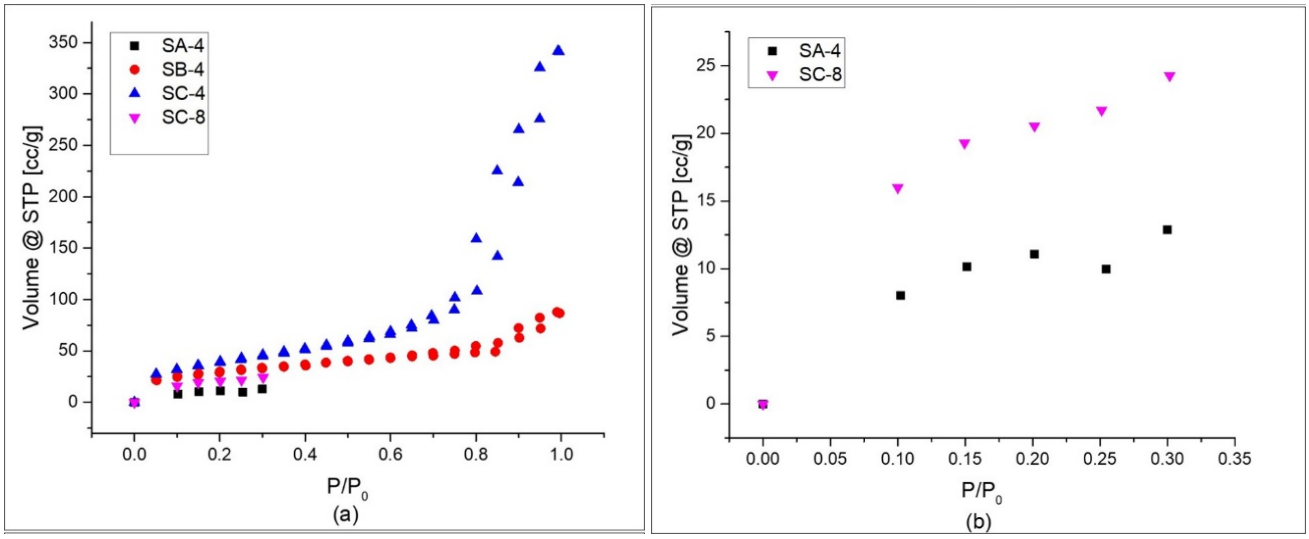

Fig. 4. N_2 sorption curves of samples, (a) four samples (b) two samples

micro to macroporous, with the most volume in the mesoporous region (between 2-50 nm). Using the BET (Brunauer-Emmett-Teller) method, the surface area of samples were 38.9 m^2/g for sample A, 102.60 m^2/g for sample B, and 74.79 for sample D, lower than that reported by previous research [30], and 141.01 m^2/g for sample C.

The adsorption-isotherm curves of samples B and C (Fig. 4a) exhibited a convergent curve. This demonstrates an indication of a multilayer formation in the adsorption process. Based on the IUPAC classification, this curve belongs to type III adsorption-isotherm. In the process, the interactions between the adsorbate molecules are greater than the adsorbents-adsorbates interaction. In both samples, capillary condensation was demonstrated by Hysteresis type H3 (at $P/P_0 \sim 0.5$-0.99 for sample C and $P/P_0 \sim 0.7$-0.99 for sample B) as a representation of mesopores-macropores with slightly micropore. This hysteresis also shows the aggregate of particles that create pores or macropores but are not filled with condensate [41].

Interestingly, the difference in the concentration of NaOH solution has a great influence on the adsorption capacity. The curve shows that sample C has a much higher

adsorption capacity than others following with the surface area of sample C which is also the largest. This is the evidence of the relationship between the measured adsorption capacity and the percentage of the pore volume. It is seen from Figure 3, although the peak of the pore volume of sample B presences at a smaller pore diameter, the percentage of volume pore of sample C is the first closest to 100% at D~ 15 nm. For two other samples, which are samples A and D (Fig. 4b), are more likely to fit type II adsorption isotherm for non-porous and microporous materials, with a monolayer mechanism due to a sharp line at first condition [16]. However, when compared to samples B and C, these two samples had finished the monolayer adsorption at low pressure and did not show a higher performance at higher pressures.

3.3. FT-IR spectra analysis

The FTIR spectra of silica from SBRHA are presented in Figure 5 and show the chemical functional groups of prepared samples. This analysis was observed to find some functional groups that have water affinity, as well as probably some water that had bonded on the sample. It is clearly seen that different concentrations of NaOH solution in the extraction had no significant effect on the chemical groups of samples. The dominant peak at ~1095 (point 3) possessed by each sample represented the Si-O-Si asymmetry stretching vibration [42-44]. The band that is located at ~470 cm^{-1} (5), ~800nm^{-1} (4), and ~3436 cm^{-1} (1) denoted to Si–O symmetry bending vibration and stretching vibration, SiO-H asymmetry stretching vibration, respectively [42-44]. At a wavenumber of ~1640 (2), a peak with low transmittance was found as ascribed to H-O-H bending vibration. The broadband at point 1 and peak at point 2 were assigned to the moisture-enriched surface of amorphous silica, which is matching with O-H bonding as the result [43]. Similar to the previous research, these spectra patterns of silica from SBRHA are identic with commercial silica from Aldrich (99.5%) [44]. In more detail, sample B shows the highest transmittance peak indicating more silica formation [45].

3.4. Water vapor adsorption analysis

Figure 6. exhibits the plot from the gravimetric measurement of water vapor adsorption capacity of four silica samples synthesized from SBRHA, along with the prediction from the obtained equation in Table 2. From the experimental results, the plots show a different relationship between the adsorbed water at every gram of silica (q) and relative humidity (RH). It is shown that the adsorption process of each material has a similar mechanism. In the lower relative humidity (below 30%), there is no significant effect of increasing humidity. In contrast, at higher relative humidity, which is in the more humid conditions (recorded at RH > 70%), a large amount of water adsorbed was observed,

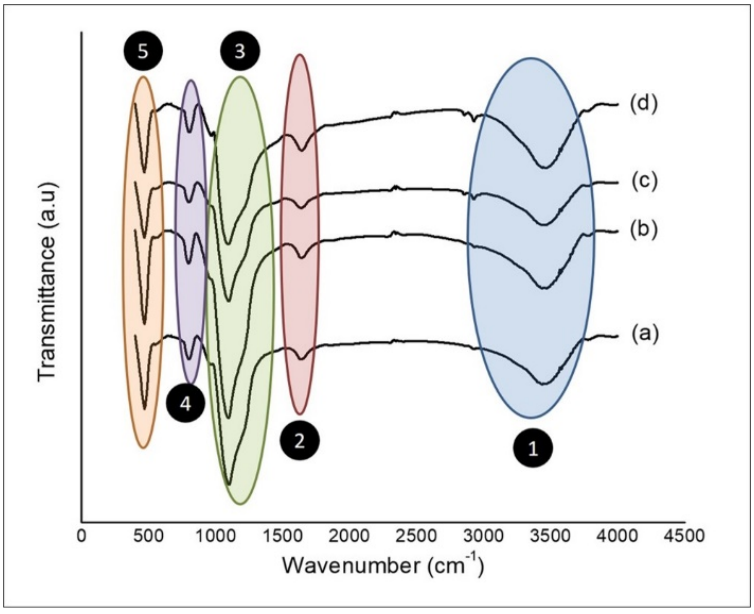

Fig. 5. FT-IR spectra of (a) sample A, (b) sample B, (c) sample C, and (d) sample D

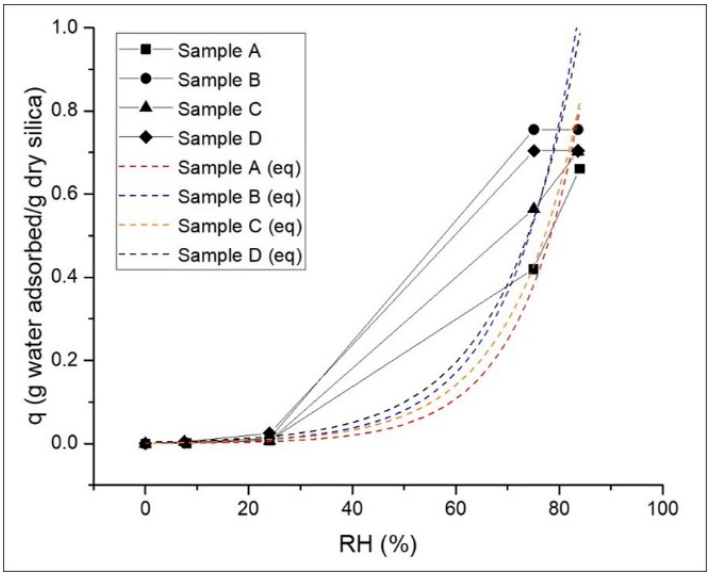

Fig. 6. Water uptake at different relative humidity from the experiment (scattered lines) and equation (dashed lines)

and these values were higher from previous research [46] and no lower than the commercial silica gels [10]. The transition of slow adsorption to the faster indicates a transition from monolayer to multilayer water adsorption and water molecular clustering has occurred. This transition took place at the humidities ranging between 24 and 75%, which suggested a critical humidity between these two points. The critical humidity shows two areas: (1) below the critical humidity, the moisture uptake was low and (2) above the critical humidity, there is a high moisture uptake as a consequence of multilayer adsorption [46]. This condition is in agreement with the result of N_2 adsorption isotherm showed in Figure 4, which means that water vapor adsorption was taken place in the mesopores-macropores particles. Particularly, for samples A and D, the water uptake remained constant after this higher RH environment, while on others still occurred van der Waals bonding between adsorbate molecules.

Table 2.
Constants of equations correlating moisture uptake at various relative humidities

Sample	Equation	R^2
A	$q = 0.0007exp^{0.0839(RH)}$	0.9895
B	$q = 0.0018exp^{0.0758(RH)}$	0.9888
C	$q = 0.0017exp^{0.0736(RH)}$	0.9841
D	$q = 0.0034exp^{0.0675(RH)}$	0.9774

Using Microsoft excel application, the equation of each water adsorption trendline was recorded as tabulated in the Table 2. The equation is defined as exponential equations. However, this equation does not perfectly fit with the water adsorption data plot, except for the first three points (low humidity). According to the adsorption isotherm type, the plots from equations are categorized as Type III that represents water clustered on the surface of nonporous or microporous solid.

4. Conclusions

Silica from semi-burned rice husk ash has been successfully prepared using the sol-gel method with various treatments in the extraction and gelation steps. In the extraction process, various concentrations of NaOH solutions were used to leached the semi-burned rice husk ash (SBRHA), while in the gelation process, two pH values were investigated (5 and 7) for sample treated with 5% of NaOH solutions. According to the results, different treatments for preparing silica from SBRHA from the formation of sodium silicate solution and silica gel process have no significant effects on the properties of the products. Based on the morphological analysis, the characteristics of the silica surface are micrometer-sized silica with large porous and addition of some agglomerated nanoparticles that formed pores. The pores belong to micro to macropores with the largest distribution consist of mesopores. The adsorption

isotherm characteristics of each sample show multilayer adsorptions indicates a strong bond between adsorbate molecules.

Acknowledgements

This research is fully funded by the Directorate General of Learning and Student Affairs, Ministry of Education and Culture, Republic of Indonesia, under schema of Outstanding Student Program Contract Number 642-03/UN7.6.1/PP/2020.

References

[1] Y. Artioli, Adsorption, in: Encyclopedia of Ecology, Five-Volume Set, 2008, 60-65.

[2] H. Hu, K. Xu, Physicochemical technologies for HRPs and risk control, in: H. Ren, X. Zhang (Eds.), High-Risk Pollutants in Wastewater, Elsevier, 2020, 169-207. DOI: https://doi.org/10.1016/B978-0-12-816448-8.00008-3

[3] M. Djaeni, P.V. Bartels, J.P.M. Sanders, G. van Straten, A.J.B. van Boxtel, Computational fluid dynamics for multistage adsorption dryer design, Drying Technology 26/4 (2008) 487-502. DOI: https://doi.org/10.1080/07373930801929532

[4] M. Djaeni, S.B. Sasongko, A. Prasetyaningrum, X. Jin, A.J. van Boxtel, Carrageenan drying with dehumidified air: Drying characteristics and product quality, International Journal of Food Engineering 8/3 (2012) 32. DOI: https://doi.org/10.1515/1556-3758.2682

[5] P. Aprea, B. de Gennaro, N. Gargiulo, A. Peluso, B. Liguori, F. Iucolano, D. Caputo, Sr-, Zn- and Cd-exchanged zeolitic materials as water vapor adsorbents for thermal energy storage applications, Applied Thermal Engineering 106 (2016) 1217-1224. DOI: https://doi.org/10.1016/j.applthermaleng.2016.06.066

[6] A. Galarneau, M. Nader, F. Guenneau, F. Di Renzo, A. Gedeon, Understanding the stability in water of mesoporous SBA-15 and M CM-41, Journal of Physical Chemistry C 111/23 (2007) 8268-8277. DOI: https://doi.org/10.1021/jp068526e

[7] Qiongfen Yu, Huirong Zhao, Hong Zhao, Shengnan Sun, Xu Ji, Ming Li, Yunfeng Wang, Preparation of tobacco-stem activated carbon from using response surface methodology and its application for water vapor adsorption in solar drying system, Solar Energy 177 (2019) 324-336. DOI: https://doi.org/10.1016/j.solener.2018.11.029

[8] A.J. Fletcher, Y. Uygur, K. Mark Thomas, Role of surface functional groups in the adsorption kinetics of water vapor on microporous activated carbons, Journal of Physical Chemistry C 111/23 (2007) 8349-8359. DOI: https://doi.org/10.1021/jp070815v

[9] S.K. Wahono, A. Suwanto, D.J. Prasetyo, Hernawan, T.H. Jatmiko, K. Vasilev, Plasma activation on natural mordenite-clinoptilolite zeolite for water vapor adsorption enhancement, Applied Surface Science 483 (2019) 940-946. DOI: https://doi.org/10.1016/j.apsusc.2019.04.033

[10] S. Saliba, P. Ruch, W. Volksen, T.P. Magbitang, G. Dubois, B. Michel, Combined influence of pore size distribution and surface hydrophilicity on the water adsorption characteristics of micro- and mesoporous silica, Microporous and Mesoporous Materials 226 (2016) 221-228. DOI: https://doi.org/10.1016/j.micromeso.2015.12.029

[11] E. David, C. Sandru, A. Armeanu, Zeolitization characteristics of fly ash and its use to manufacture porous materials, Archives of Materials Science and Engineering 90/2 (2018) 56-67. DOI: https://doi.org/10.5604/01.3001.0012.0663

[12] E.T. Wahyuni, R. Roto, F.A. Nissah, Mudasir, N.H. Aprilita, Modified silica adsorbent from volcanic ash for Cr(VI) anionic removal, Indonesian Journal of Chemistry 18/3 (2018) 428-433. DOI: https://doi.org/10.22146/ijc.26905

[13] A. Sdiri, T. Higashi, S. Bouaziz, M. Benzina, Synthesis and characterization of silica gel from siliceous sands of southern Tunisia, Arabian Journal of Chemistry 7/4 (2014) 486-493. DOI: https://doi.org/10.1016/j.arabjc.2010.11.007

[14] S. Sun, Q. Yu, M. Li, H. Zhao, C. Wu, Preparation of coffee-shell activated carbon and its application for water vapor adsorption, Renewable Energy 142 (2019) 11-19. DOI: https://doi.org/10.1016/j.renene.2019.04.097

[15] R. Wang, Y. Amano, M. Machida, Surface properties and water vapor adsorption-desorption characteristics of bamboo-based activated carbon, Journal of Analitycal and Applied Pyrolysis 104 (2013) 667-674. DOI: https://doi.org/10.1016/j.jaap.2013.04.013

[16] M. Thommes, K. Kaneko, A.V. Neimark, J.P. Olivier, F. Rodriguez-Reinoso, J. Rouquerol, K.S.W. Sing, Physisorption of gases, with special reference to the evaluation of surface area and pore size distribution (IUPAC Technical Report), Pure and Applied Chemistry 87/9-10 (2015) 1051-1069. DOI: https://doi.org/10.1515/pac-2014-1117

[17] K.M. Kim, H.T. Oh, S.J. Lim, K. Ho, Y. Park, C.H. Lee, Adsorption Equilibria of Water Vapor on Zeolite 3A, Zeolite 13X, and Dealuminated y Zeolite, Journal of Chemical & Engineering Data 61/4 (2016) 1547-1554. DOI: https://doi.org/10.1021/acs.jced.5b00927
[18] A. Centineo, H.G.T. Nguyen, L. Espinal, J.C. Horn, S. Brandani, An experimental and modelling study of water vapour adsorption on SBA-15, Microporous and Mesoporous Materials 282 (2019) 53-72. DOI: https://doi.org/10.1016/j.micromeso.2019.03.018
[19] M. Djaeni, P. Bartels, J. Sanders, G. van Straten, A.J. B. van Boxtel, Process integration for food drying with air dehumidified by zeolites, Drying Technology 25/1 (2007) 225-239. DOI: https://doi.org/10.1080/07373930601161096
[20] M. Djaeni, A.M. Perdanianti, The study explores the effect of onion (allium cepa l.) drying using hot air dehumidified by activated carbon, silica gel and zeolite, Journal of Physics: Conference Series 1295 (2019) 012025. DOI: https://doi.org/10.1088/1742-6596/1295/1/012025
[21] L. Xin, L. Huiling, H. Siqi, L. Zhong, Dynamics and isotherms of water vapor sorption on mesoporous silica gels modified by different salts, Kinetics and Catalysis 51/5 (2010) 754-761. DOI: https://doi.org/10.1134/S0023158410050186
[22] H. Negishi, A. Miyamoto, A. Endo, Preparation of thick mesoporous silica coating by electrophoretic deposition with binder addition and its water vapor adsorption-desorption properties, Microporous and Mesoporous Materials 180 (2013) 250-256. DOI: https://doi.org/10.1016/j.micromeso.2013.06.040
[23] P. Velmurugan, J. Shim, K.-J. Lee, M. Cho, S.-S. Lim, S.-K. Seo, K.-M. Cho, K.-S. Bang, B.-T. Oh, Extraction, characterization, and catalytic potential of amorphous silica from corn cobs by sol-gel method, Journal of Industrial and Engineering Chemistry 29 (2015) 298-303. DOI: https://doi.org/10.1016/j.jiec.2015.04.009
[24] R.A. Bakar, R. Yahya, S.N. Gan, Production of High Purity Amorphous Silica from Rice Husk, Procedia Chemistry 19 (2016) 189-195. DOI: https://doi.org/10.1016/j.proche.2016.03.092
[25] T.H. Liou, C.C. Yang, Synthesis and surface characteristics of nanosilica produced from alkali-extracted rice husk ash, Materials Science and Engineering: B 176/7 (2011) 521-529. DOI: https://doi.org/10.1016/j.mseb.2011.01.007
[26] A. Mahmud, P.S.M. Megat-Yusoff, F. Ahmad, A.A. Farezzuan, Acid leaching as efficient chemical treatment for rice husk in production of amorphous silica nanoparticles, ARPN Journal of Engineering and Applied Sciences 11/22 (2016) 13384-13388.
[27] H.X. Nguyen, N.T.T. Dao, H.T.T. Nguyen, A.Q.T. Le, Nanosilica synthesis from rice husk and application for soaking seeds, IOP Conference Series: Earth and Environmental Science 266/1 (2019) 012007. DOI: https://doi.org/10.1088/1755-1315/266/1/012007
[28] S. Shekar, M. Sander, R.C. Riehl, A.J. Smith, A. Braumann, M. Kraft, Modelling the flame synthesis of silica nanoparticles from tetraethoxysilane, Chemical Engineering Science 70 (2012) 54-66. DOI: https://doi.org/10.1016/j.ces.2011.06.010
[29] H. Yoo, J. Pak, Synthesis of highly fluorescent silica nanoparticles in a reverse microemulsion through double-layered doping of organic fluorophores, Journal of Nanoparticle Research 15/5 (2013) 1609. DOI: https://doi.org/10.1007/s11051-013-1609-2
[30] S. Azat, A.V. Korobeinyk, K. Moustakas, V.J. Inglezakis, Sustainable production of pure silica from rice husk waste in Kazakhstan, Journal of Cleaner Production 217 (2019) 352-359. DOI: https://doi.org/10.1016/j.jclepro.2019.01.142
[31] K.V. Selvakumar, A. Umesh, P. Ezhilkumar, S. Gayatri, P. Vinith, V. Vignesh, Extraction of silica from burnt paddy husk, International Journal of ChemTech Research 6/9 (2014) 4455-4459.
[32] R.R. Zaky, M.M. Hessien, A.A. El-midany, M.H. Khedr, Preparation of silica nanoparticles from semi-burned rice straw ash, Powder Technology 185 (2008) 31-35. DOI: https://doi.org/10.1016/j.powtec.2007.09.012
[33] P.M. Doran, Introduction to Engineering Calculations, in: Bioprocess Engineering Principles, Second Edition, Academic Press, Oxford, 2013, 13-44.
[34] C. Bourgault, P. Lessard, C. Remington, C.C. Dorea, Experimental Determination of Moisture Sorption Isotherm of Fecal Sludge, Water 11/2 (2019) 303. DOI: https://doi.org/10.3390/w11020303
[35] L. Greenspan, Humidity fixed points of binary saturated aqueous solutions, Journal of Research of the National Bureau of Standards – A. Physics and Chemistry 81/1 (1977) 89-96.
[36] S.B. Daffalla, H. Mukhtar, M.S. Shaharun, Characterization of adsorbent developed from rice husk: Effect of surface functional group on phenol adsorption, Journal of Applied Science 10/12 (2010) 1060-1067. DOI: https://doi.org/10.3923/jas.2010.1060.1067
[37] M.M. Saravanan, M. Sivaraja, Mechanical behavior of concrete modified by replacement of cement by rice

husk ash, Brazilian Archives of Biology and Technology 59/S2 (2016) 1-11.
DOI: http://dx.doi.org/10.1590/1678-4324-2016161072
[38] I.M. Joni, L. Nulhakim, M. Vanitha, C. Panatarani, Characteristics of crystalline silica (SiO_2) particles prepared by simple solution method using sodium silicate (Na_2SiO_3) precursor, Journal of Physics: Conference Series 1080 (2018) 012006. DOI: https://doi.org/10.1088/1742-6596/1080/1/012006
[39] I.C. Medeiros-Costa, C. Laroche, J. Pérez-Pellitero, B. Coasne, Characterization of hierarchical zeolites: Combining adsorption/intrusion, electron microscopy, diffraction and spectroscopic techniques, Microporous and Mesoporous Materials 287 (2019) 167-176. DOI: https://doi.org/10.1016/j.micromeso.2019.05.057
[40] J. Zecevic, C.J. Gommes, H. Friedrich, P.E. de Jongh, K.P. de Jong, Mesoporosity of Zeolite Y: Quantitative Three-Dimensional Study by Image Analysis of Electron Tomograms, Angewandte Chemie International Edition 51/17 (2012) 4213-4217.
DOI: https://doi.org/10.1002/anie.201200317
[41] K.S.W. Sing, R.T. Williams, Physisorption hysteresis loops and the characterization of nanoporous materials, Adsorption Science and Technology 22/10 (2004) 773-782. DOI: https://doi.org/10.1260/0263617053499032
[42] Y. Liu, Y. Guo, Y. Zhu, D. An, W. Gao, Z. Wang, Y. Ma, Z. Wang, A sustainable route for the preparation of activated carbon and silica from rice husk ash, Journal of Hazardous Materials 186/2-3 (2011) 1314-1319.
DOI: https://doi.org/10.1016/j.jhazmat.2010.12.007
[43] Musyarofah, S. Soontaranon, W. Limphirat, Triwikantoro, S. Pratapa, XRD, WAXS, FTIR, and XANES studies of silica-zirconia systems, Ceramics International 45/12 (2019) 15660-15670.
DOI: https://doi.org/10.1016/j.ceramint.2019.05.078
[44] P. Lu, Y. Hsieh, Highly pure amorphous silica nano-disks from rice straw, Powder Technology 225 (2012) 149-155.
DOI: https://doi.org/10.1016/j.powtec.2012.04.002
[45] T. Liou, Preparation and characterization of nano-structured silica from rice husk, Materials Science and Engineering: A 364/1-2 (2004) 313-323. DOI: https://doi.org/10.1016/j.msea.2003.08.045
[46] H. Zhang, W. Gu, M.J. Li, Z.Y. Li, Z.J. Hu, W.Q. Tao, Experimental study on the kinetics of water vapor sorption on the inner surface of silica nano-porous materials, International Journal of Heat and Mass Transfer 78 (2014) 947-959. DOI: https://doi.org/10.1016/j.ijheatmasstransfer.2014.07.047